Domain-Selective Ligand-Binding Modes and Atomic Level Pharmacophore Refinement in Angiotensin I Converting Enzyme (ACE) Inhibitors

Andreas G. Tzakos and Ioannis P. Gerothanassis*[a]

Somatic ACE (EC 3.4.15.1), a Zn^{II} metalloproteinase, is composed of functionally active N and C domains resulting from tandem gene duplication. Despite the high degree of sequence similarity between the two domains, they differ in substrate and inhibitor specificity and in their activation by chloride ions. Because of the critical role of ACE in cardiovascular and renal diseases, both domains are attractive targets for drug design. Putative structural models have been generated for the interactions of ACE inhibitors (lisinopril, captoril, enalaprilat, keto-ACE, ramiprilat, quinaprilat, peridoprilat, fosinoprilat, and RXP 407) with both the ACE_C and the ACE_N domains. Inhibitor-domain selectivity was interpreted in terms of residue alterations observed in the four subsites of the binding grooves of the ACE_C/ACE_N domains (S1: V516/N494, V518/T496, S2: F391/Y369, E403/R381, S1′: D377/Q355, E162/D140, V379/S357, V380/T358, and S2′: D463/E431, T282/S260). The interactions governing the ligand–receptor recognition process in the ACE_C domain are: a salt bridge between D377, E162, and the NH_2 group (P1′ position), a hydrogen bond of the inhibitor with Q281, the presence of bulky hydrophobic groups in the P1 and P2′ sites, and a stacking interaction of F391 with a benzyl group in the P2 position. In ACE_N these interactions are: hydrogen bonds of the inhibitor with E431, Y369, and R381, and a salt bridge between the carboxy group in the P2 position of the inhibitor and R500. The calculated complexes were evaluated for their consistency with structure–activity relationships and site-directed mutagenesis data. A comparison between the calculated interaction free energies and the experimentally observed biological activities was also made. Pharmacophore refinement was achieved at an atomic level, and might provide an improved basis for structure-based rational design of second-generation, domain-selective inhibitors.

Introduction

Somatic ACE (EC 3.4.15.1) has two metalloproteinase domains (known as N (ACE_N) and C (ACE_C)), each containing a canonical Zn^{II}-binding sequence motif—HExxH (His-Glu-x-x-His)[1]—as the result of a tandem gene duplication, with each domain possessing a functional active site.[2,3] Since the discovery that ACE has two active sites, there has been much speculation about their functional significance. Although in vitro the two domains of ACE display a relatively broad substrate specificity, such as the ability to cleave angiotensin I (AI) and bradykinin (BK), there are some biochemical features that differentiate between the two active sites.[3–7] For example, the hematoregulatory peptide *N*-acetyl-seryl-aspartyl-lysyl-proline (Ac-SDKP) was shown to be specifically cleaved in vitro by the N domain of ACE.[8] Another specific substrate for the N domain is angiotensin 1–7 (D-R-V-Y-I-H-P), although this peptide also inhibits the hydrolysis of angiotensin I by the C domain.[7] The activity of the C-terminal domain is highly dependent on chloride ion concentration, whereas the N-terminal domain is still active in the absence of chloride and is fully activated at relatively low concentrations of this anion.[2,4] The N active site is preferentially involved in the N-terminal endopeptidase cleavage of LH-RH, but with low catalytic efficiency.[4] Captopril, lisinopril, and RXP 407 display different inhibitory potencies towards the two active sites.[3,9–11] These data therefore suggest that some structural differences occur between the two active sites of ACE.

Because of its central role in the metabolism of vasoactive peptides and since the ACE gene is a candidate for several cardiovascular diseases, ACE has attracted intense interest for the development of orally active ACE inhibitors to treat hypertension.[12] The demonstration that the physiological functions of ACE are not limited to its cardiovascular role[8,11,13] have increased interest in studies of domain specificity and inhibition.[6,9]

Inhibitors of ACE are effective and widely used drugs for therapy for hypertension, heart disease, diabetic neuropathy, and atherosclerosis.[14,15] One major problem in the design of strong and selective ACE inhibitors in the past has been the lack of detailed structural information on the interaction between ACE and its inhibitors. The design of the first generation inhibitors (captopril, enalaprilat, and lisinopril) was extended and 17 ACE inhibitors have been approved for clinical use.[16] The later compounds are all variations on the original scheme,

[a] *A. G. Tzakos, Prof. I. P. Gerothanassis*
Section of Organic Chemistry and Biochemistry
Department of Chemistry, University of Ioannina
45110, Ioannina (Greece)
Fax: (+30) 265-109-8799
E-mail: igeroth@cc.uoi.gr

Supporting information for this article is available on the WWW under http://www.chembiochem.org or from the author.

 DOI: 10.1002/cbic.200400386

with most of the differences residing in the functional groups that bind the active-site zinc(II) and the S2′ pocket.[14]

In cases in which the target receptor structure is unknown, (Q)SAR and pharmacophore-based approaches often assist in the adoption of rational design strategies. Until recently, drug design efforts for ACE relied on pharmacophore hypotheses derived from the structures of the active sites of other carboxypeptidases. Extensive pharmacophore and 3D-QSAR studies, performed by Marshall et al.,[17,18] were based on the hypothesis that all classes of ligands bind to the active-site zinc(II) by the same mode, and the basic structural requirements for inhibition of ACE involve: i) a terminal carboxyl group, ii) an amido carbonyl group, and iii) different types of effective zinc(II) ligand functional groups. From these studies, an active-site model generally in accordance with the experimental data was developed.

Although the literature pharmacophore hypotheses were successful for the development of highly potent ligands, there remain many uncertainties about the details of the ligand–receptor interactions. Protein-based virtual screening should be more efficient than the pharmacophore-based method for the rational design of receptor-specific drugs, since the protein environment of the ligand is taken into account, thus giving access to intermolecular interactions responsible for the ligand–receptor molecular recognition.

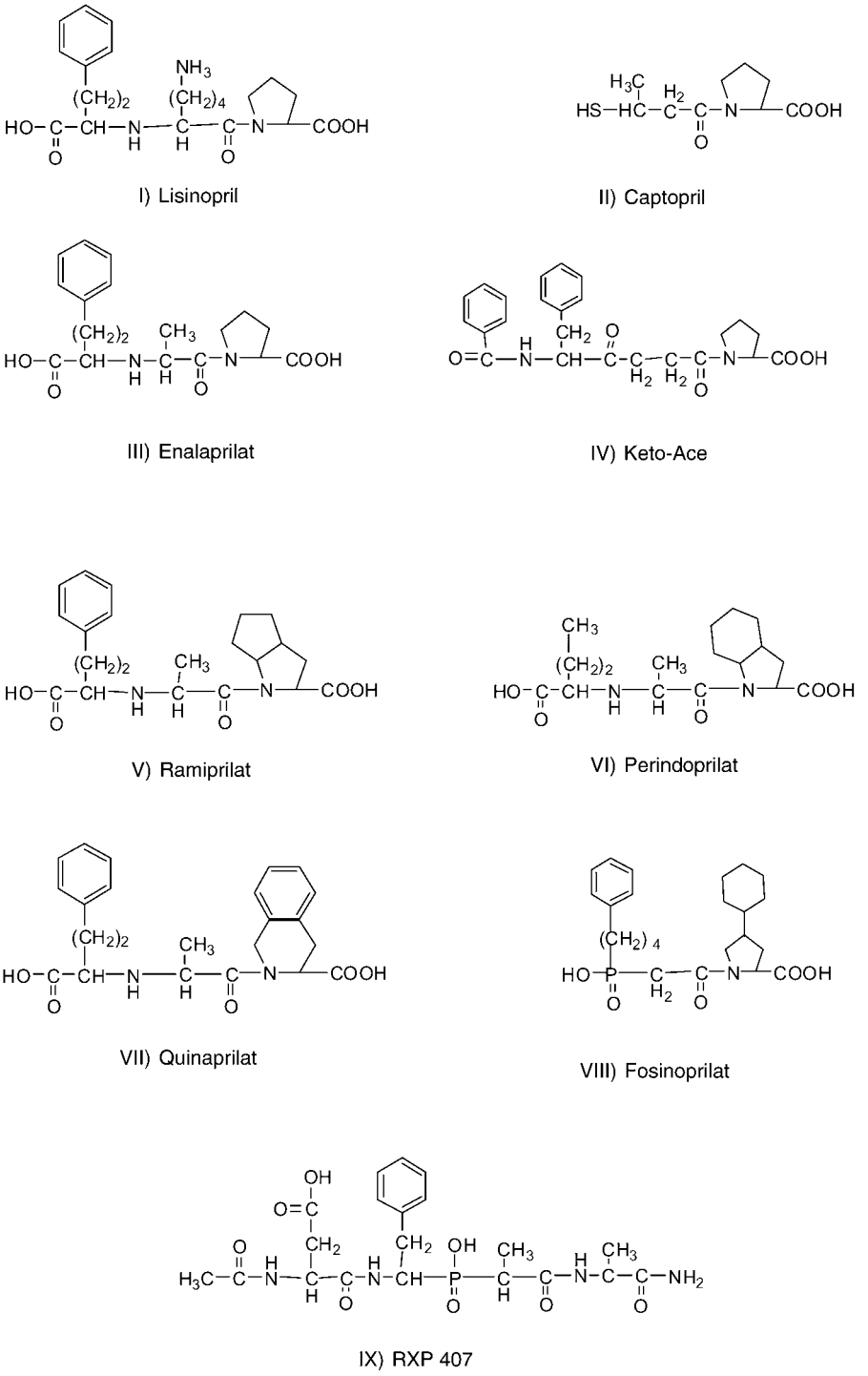

Scheme 1. Chemical structures of the investigated ACE inhibitors.

Here we report docking studies of several selective ACE_C and ACE_N inhibitors, based on the recently published high-resolution X-ray structures of captopril, lisinopril, and enalaprilat with *t*ACE complexes,[19,20] and the structure of ACE_N constructed through homology modeling.[21] In order to understand the ACE–inhibitor interactions better, we have chosen nine nonpeptidic compounds with diversity in their inhibitory potencies and the chemical structures shown in Scheme 1. Moreover, for the first time, correlation between the biological activities of ACE inhibitors and calculated ligand–protein interaction energies was investigated and the pharmacophoric requirements of the ligands were defined on an atomic level structural basis. The structural insights provided by this study should enhance understanding of the factors controlling the selectivity of the two domains of *s*ACE and should constitute solid bases for the design of new selective ACE inhibitors.

Results and Discussion

Comparison of the structural features of ACE inhibitors in the unbound state

It is interesting to compare the structural features of the inhibitors in the unbound state and to investigate structural modifications upon binding to the enzymic binding groove. A superposition of the crystallographic structures, retrieved from the Cambridge Crystallographic Database (CCD), of seven ACE inhibitors (captoril, enalaprilat, keto-ACE, ramiprilat, quinaprilat, peridoprilat, and fosinoprilat) in their unbound states was achieved by aligning the relative amide groups of the inhibitors (Figure 1). It is noteworthy that the crystal structures of these

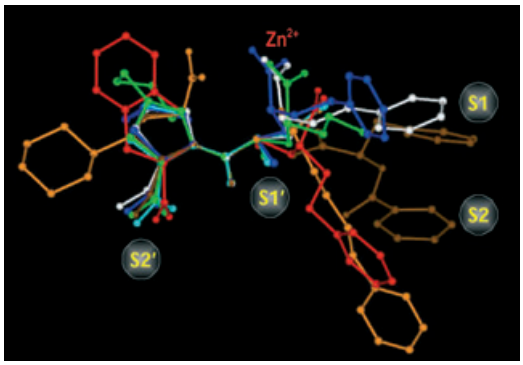

Figure 1. Superposition of the X-ray structures of the unbound ligands: captopril (cyan), enalaprilat (white), ramiprilat (blue), quinaprilat (red), peridoprilat (green), fosinoprilat (orange) and keto-ACE (brown).

molecules, which have similar anchoring sites, exhibit comparable relative orientations of the pharmacophore functional groups, regardless of the molecular environment in the crystalline state. The hydrophobic side chain (P1) is in an extended conformation, and the lengthening of the P2′ chain by bulky hydrophobic groups in **V**–**VII** and in **VIII** does not change its conformation. The side chains of the P1 group of the inhibitors fosinoprilat and quinaprilat and the P2 group of keto-ACE form one cluster of common orientation, whilst ramiprilat, perindoprilat, keto-ACE (P1 group), and enalaprilat form a different cluster of common orientation. The relative orientations of the two carboxy groups, on opposite side of the amido plane, are very similar, except in the case of fosinoprilat (**VIII**; depicted in orange in Figure 1).

Docking calculations for inhibitors I–IX in the two catalytic domains of the *s*ACE enzyme

The substrate-binding site of ACE_N and ACE_C of somatic ACE and of the Drosophila AnCE and ACE2 isoforms is a large continuous internal channel composed of two chambers of unequal size. The larger chamber is the binding site of the amino-terminal eight amino acids of the substrate angiotensin I, and has been referred to as the "N-chamber", whilst the carboxy dipeptide portion of the substrate binds to the smaller chamber and has been referred to as the "C-chamber".[22] These spacious chambers are sufficiently large for the binding of short substrate peptides. The catalytic zinc(II) and inhibitor binding sites are located in the narrow bottleneck connecting the two chambers ≈10 Å from the entrance. The substrate-binding channel of ACE_C is predominantly negatively charged, whilst that in ACE_N is less negatively charged.[21] The N- and C-chambers are open to the exterior solvent area through narrow holes with approximate diameters of 3 Å, which appear to be too small for the passage of peptide substrates. Flexibility and "breathing" motions of the opening holes are probably required for efficient catalysis.

Docking of the compounds **I**–**IX** revealed a consistent network of ionic and hydrogen bonds between the ligand and the enzyme side chains. The most important interactions found for each compound are summarized in Table 1 and Table 2. The inhibitors cannot fill up the spacious substrate-

Table 1. Result of 50 independent docking runs for each ligand in ACE_C.

Ligand	E[a]	K_{iC}[b] [nM]	IC_{50C}[b]	Surrounding residues
Lisinopril	−16.6	0.24[2,3]		E162, Q281, **H353**, **A354**, S355, D377, V380, H383, E384, H387, E411, F457, **K511**, F512, **H513**, S516, V518, **Y520**, **Y523**, F527
Captopril	−7.2	1.4[3,10,24]		Q281, **H353**, **A354**, V380, H383, E384, H387, E411, F457, **K511**, **H513**, **Y520**, **Y523**, F527
Enalaprilat	−14.8	0.63[2]		Q281, **H353**, **A354**, S355, V380, H383, E384, H387, E411, F457, **K511**, F512, **H513**, S516, V518, **Y520**, **Y523**
keto-ACE	−13.0		0.04[7,27]	Q281, **H353**, S355, **A356**, V380, H383, E384, H387, F391 E411, F457, **K511**, F512, **H513**, S516, V518, **Y520**, **Y523**
Ramiprilat	−14.8			Q281, T282, **H353**, **A354**, S355, V380, H383, E384, H387, E411, D453, F457, **K511**, F512, **H513**, S516, V518, **Y520**, **Y523**, F527
Peridoprilat	−15.2			Q281, T282, **H353**, **A354**, S355, V380, H383, E384, H387, E411, D453, F457, F460, **K511**, F512, **H513**, S516, V518, **Y520**, **Y523**, F527
Quinaprilat	−15.3			Q281, T282, **H353**, **A354**, S355, V379, V380, H383, E384, H387, E411, D453, F457, F460, **K511**, F512, **H513**, S516, V518, **Y520**, **Y523**, F527
Fosinoprilat	−16.7			Q281, T282, V351, **H353**, S355, W357, K368, V379, V380, H383, E384, H387, E411, D415, D453, K454, F457, F460, **K511**, F512, **H513**, S516, V518, **Y520**, **Y523**, F527, Q530
RXP 407	−14.0	7500[9]		Q281, V351, **H353**, S355, **A356**, W357, K368, V379, V380, H383, E384, H387, F391, H410, E403, E411, D453, F457, **K511**, F512, **H513**, S516, V518, **Y520**, **R522**, **Y523**, F527

[a] E is the estimated free energy of binding for the best cluster results and is given in kcal mol^{-1}. The last column shows the residues of the binding site located within 5 Å of any atom of the docked ligands. Residues that form hydrogen bonds with the ligand are highlighted in bold, and residues that differ in ACE_C and in ACE_N are underlined. [b] K_{iC} and IC_{50C} values reported according to the literature.

Table 2. Results of 50 independent docking runs for each ligand in ACE_N

Ligand	E[a]	K_{iN}[b] [nM]	IC_{50N}[b]	Surrounding residues
Lisinopril	−15.7	4.4[2,3]		D140, Q259, **H331**, **A332**, S333, Q355, T358, H361, E362, H365, E389, F435, **K489**, F490, **H491**, N494, T496, **Y498**, **Y501**, F505
Captopril	−7.0	0.89[3,10,24]		Q259, **H331**, **A332**, T358, H361, E362, H365, E389, F435, **K489**, **H491**, **Y498**, **Y501**, F505
Enalaprilat	−14.7	2.6[2]		Q259, **H331**, **A332**, S333, T358, H361, E362, H365, E389, F435, **K489**, F490, **H491**, N494, T496, **Y498**, **Y501**, F505
keto-ACE	−12.5		1.5[7,27]	Q259, **H331**, **A334**, W335, T358, H361, E362, H365, Y369, E389, F435, **K489**, F490, **H491**, N494, T496, **Y498**, **Y501**, F505
Ramiprilat	−14.3			Q259, S260, V329, **H331**, **A332**, S333, T358, H361, E362, H365, E389, D393, E431, F435, F438, **K489**, F490, **H491**, N494, T496, **Y498**, **Y501**, F505
Peridoprilat	−15.1			Q259, S260, V329, **H331**, **A332**, S333, T358, H361, E362, H365, E389, D393, E431, F435, F438, **K489**, F490, **H491**, N494, T496, **Y498**, **Y501**, F505
Quinaprilat	−14.7			Q259, S260, V329, **H331**, **A332**, S333, S357, T358, H361, E362, H365, E389, D393, E431, F435, F438, **K489**, F490, **H491**, N494, T496, **Y498**, **Y501**, F505
Fosinoprilat	−16.5			Q259, S260, V329, **H331**, S333, W335, K346, S357, T358, H361, E362, H365, E389, D393, E431, K432, F435, **K489**, F490, **H491**, N492, T494, **Y498**, **Y501**, F505, Q508
RXP 407	−17.0	7.0[9]		Q259, V329, **H331**, S333, **A334**, W335, K346, S357, T358, H361, E362, H365, **Y369**, **R381**, H388, E389, E431, F435, **K489**, F490, **H491**, N494, T496, **Y498**, **Y501**, **R500**, F505

[a] E is the estimated free energy of binding for the best cluster results and is given in kcal mol^{-1}. The last column shows the residues of the binding site located within 5 Å of any atom of the docked ligands. Residues forming hydrogen bonds with the ligand are highlighted in bold and residues that differ in ACE_C and in ACE_N are underlined. [b] K_{iN} and IC_{50N} values reported according to literature.

binding channel and the shape of the inhibitors or substrates appears to have a minor role in determining specificity of the enzyme. ACE generally favors a hydrophobic residue at the carboxy-terminus of the substrate. The binding surface of the carboxy-terminal proline moieties of the inhibitors is composed of a hydrophobic patch provided by residues F457/F435, F527/F505, Y520/Y498, and Y523/Y501 (ACE_C/ACE_N). This conserved patch is involved in the binding of bulky hydrophobic residues, such as isoleucines or phenylalanines, in ACE substrates (see also discussion below).

With the aim of testing the AutoDock program for its ability to reproduce the crystal structure of the ACE_C–inhibitor complexes, as well as for comparative purposes, lisinopril, captopril, and enalaprilat were subjected to automated docking calculations. The program was successful in reproducing the experimentally determined binding modes of the three inhibitors. A superposition of the three inhibitor complexes, derived through docking calculations, with the X-ray structures of the lisinopril–, captopril–, and enalaprilat–*t*ACE complexes is denoted in Figure S1 and gives a direct evaluation of the quality and validity of the molecular modeling. It should be noted that, although the predicted free energy of binding is a useful descriptor of ligand–receptor complementarity, the choice of the "best" docking model was ultimately also dictated by its agreement with the structure–activity relationships (SARs) and the available site-directed mutagenesis data. These are described in detail in the following section.

ACE_C– and ACE_N–proline-containing inhibitor complexes: the cases of lisinopril, captopril, enalaprilat, keto-ACE, ramiprilat, and perindoprilat

Lisinopril: Lisinopril, a tripeptide analogue of Phe-Lys-Pro, binds to human sACE with $K_i = 0.39$ nM[2] and appears to mimic peptide substrates. It is also a highly efficient inhibitor of ACE_C (K_i of 0.2 nM[3]). Both the X-ray and the calculated complexes show lisinopril buried deep inside the cavity, adjacent to the HExxH motif and the catalytic Zn^{II}. As indicated in Figure 2A, the carboxylate group located between the phenylpropyl group and the lysine binds to the active site Zn^{II} and also forms hydrogen bonds with the side chain carboxylate of E384 and the Y523 side chain hydroxy group. The phenyl ring at the amino-terminal of the inhibitor interacts with the probable S1 subsite in the active site (accommodated by aromatic stacking with F512). The lisinopril lysine moiety interacts with the S1′ subsite and is contacted by the E162 and D377 residues. The accommodation of the lisinopril carboxy-terminal proline moiety by the S2′ subsite is mediated by the hydrophobic interaction with the aromatic ring of Y520 and also through ionic interactions and hydrogen bonds with K511, Q281, and Y520.

In the case of the ACE_N–lisinopril complex (Figure 2B), the docking calculations estimated the free energy of binding $E = -15.7$ kcal mol^{-1} (Table 2) for the most populated cluster and among the first solutions. The ligand is in the same location as in the crystal structure of the ACE_C–lisinopril complex, with some alterations in ligand–protein interactions observed in the S1 and S1′ subsites, as illustrated in Figure 2.

The H513/H491 and H353/H331 (ACE_C/ACE_N) residues interact with the carbonyl oxygen of the peptide bond connecting the terminal proline and lysine moiety of lisinopril. Interestingly, a 120000-fold decrease in the binding of lisinopril was observed with the H1089 to alanine mutation in human *s*ACE,[23] corresponding to the H513 residue of ACE_C and H491 of ACE_N. This is in excellent agreement with our docking calculations (Tables 1 and 2). This interaction is observed in all the studied inhibitors for both domains.

Interestingly, docking calculations indicate that lisinopril has the higher affinity for ACE_C. This is consistent with biological experiments, which suggested that the K_i value of lisinopril is about 18 times lower for the C domain than for the N domain at high chloride concentration (300 mM [Cl^-]; Tables 1 and 2).

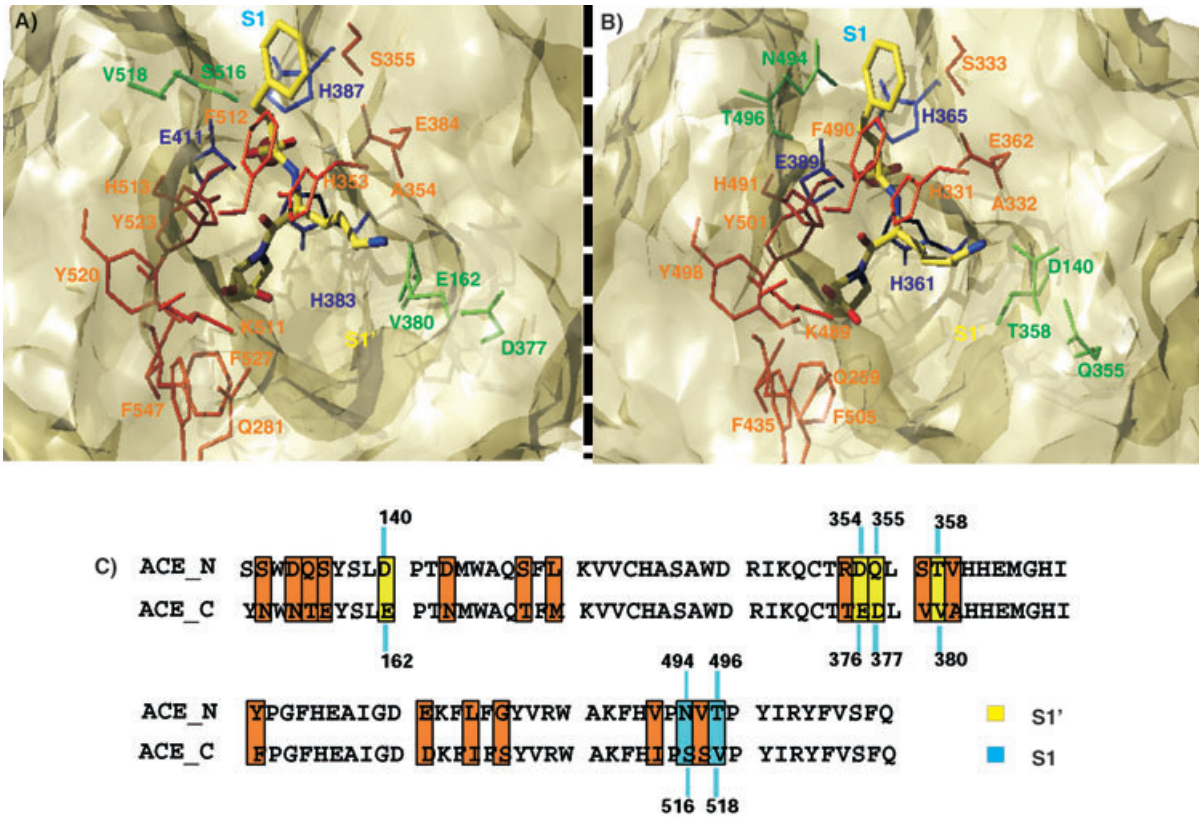

Figure 2. Binding of lisinopril (**I**) to A) the ACE_C and B) the ACE_N binding sites. C) Amino acid alignment of the residues of the two binding pockets of ACE_N and ACE_C in a cutoff of 10 Å radius around lisinopril.

In ACE_C the lysine side chain of lisinopril forms a salt bridge with D377, whereas in ACE_N Q355 is located in the same position. In addition, the E162/D140 alteration in ACE_N (ACE_C/ACE_N) results in an increased distance between the side chain of D140(OE2) and the lysine side chain (NH_2) of lisinipril; this gives rise to a lower affinity of ACE_N than of ACE_C for lisinopril.

Captopril: Captopril (Scheme 1) is the smallest competitive inhibitor of ACE, binding to human sACE with $K_i \approx 1.4$ nM,[24] and can be viewed as an N-thioalkyl derivative of the dipeptide Ala-Pro. It has been designed to mimic the two carboxy-terminal residues of the enzyme substrate. The thiol group of captopril interacts directly with the zinc(II) ion, in a distorted tetrahedral geometry (Figure 3). The carboxy-end of the proline moiety is held by three highly conserved residues—Q281/Q259, K511/K489, and Y520/Y498 (ACE_C/ACE_N)—through ionic and hydrogen bonds. These residues are also involved in binding of the carboxy-terminal proline moiety of lisinopril. The carbonyl oxygen of the peptide bond is locked by two strong hydrogen bonds with residues H513/H491 and H353/H331 (ACE_C/ACE_N). Mutation of the H1089 residue of human somatic ACE, corresponding to the H513 residue in ACE_C and H491 in ACE_N, abolishes binding of captopril and lisinopril to the enzyme.[23] Because of its small size, captopril cannot fill up the spacious substrate-binding channels either of ACE_C or of ACE_N, and the shape of the inhibitor appears to have only a minor role in determining the specificity of the enzyme. Captopril has been noted to be modestly N-selective, depending on Cl^- concentration.[3,10] This is consistent with the docking results, which gave close values for the estimated free energies of binding for ACE_C and ACE_N, of −7.2 and −7.0 kcal mol^{-1}, respectively. Captopril's differentiation between the binding grooves in ACE_C and ACE_N is due to the V380/T358 alteration (ACE_C/ACE_N) located in the S1′ subsite that accommodates the alanyl group.

Enalaprilat: Enalaprilat is a tripeptide possessing a Zn^{II}-coordinating carboxyl group and closely resembles the Phe-Ala-Pro sequence that was found to be the optimal C-terminal sequence among bradykinin potentiating factor (BPF) peptides.[25] Enalaprilat is in the same location relative to the putative binding pockets of ACE_C (Figure 4A) and ACE_N (Figure 4B) as observed in the crystal structure of the ACE_C–lisinopril complex. The binding affinity of the inhibitor at different chloride concentrations differs only modestly for the two binding domains: at high chloride concentrations (300 mM [Cl^-]) enalaprilat inhibits the C domain in preference to the N domain, with a K_i value for the C domain four times lower than that for the N domain, whilst at low chloride concentrations (20 mM [Cl^-]), enalaprilat preferentially inhibits the N domain, with a K_i value twice as low for the N domain.[2] The different inhibitor affinities observed at lower chloride concentrations could be due to a synergistic contribution by the chloride anion, through a potent structural reorientation of K511.[21] The calculations revealed very similar inhibitor affinities for the two

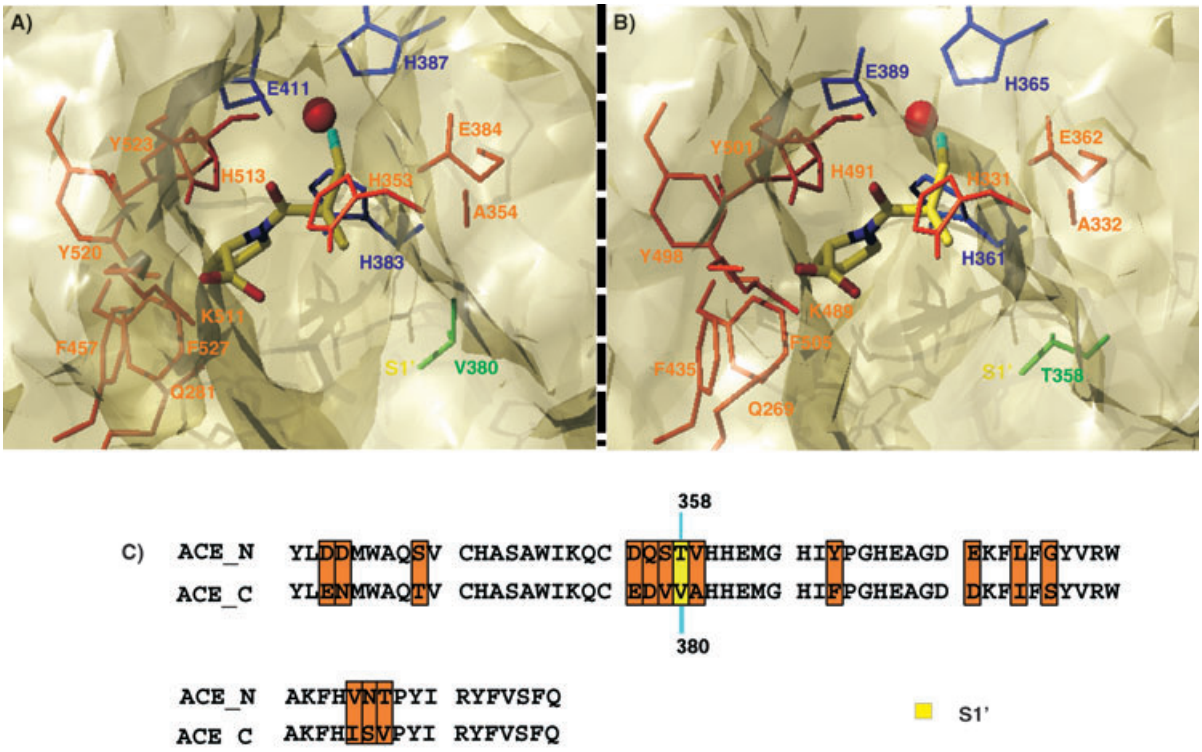

Figure 3. Binding of captopril (**II**) to A) the ACE_C, and B) the ACE_N binding sites. The thiol group of the inhibitor is shown in cyan. C) Amino acid alignment of the residues of the two binding pockets of ACE_N and ACE_C for a cutoff of 10 Å radius around captopril.

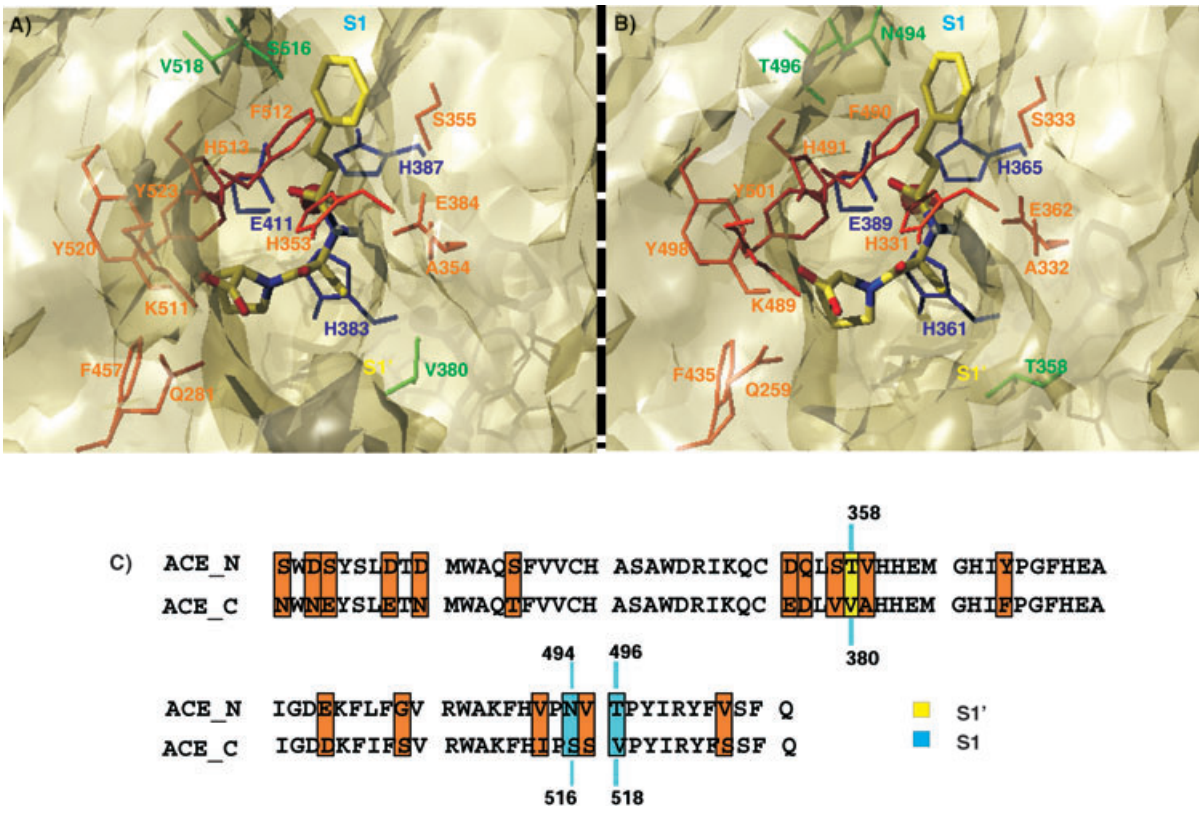

Figure 4. Binding of enalaprilat (**III**) to A) the ACE_C and B) the ACE_N binding sites. C) Amino acid alignment of the residues of the two binding pockets of ACE_N and ACE_C for a cutoff of 10 Å radius around enalaprilat.

domains (estimated free energies of binding $E = -14.8$ and -14.7 kcal mol^{-1} for the C- and N domains, respectively). Enalaprilat differs from lisinopril in the P1′ group: in lisinopril this is a lysyl group, whereas in enalaprilat it is an alanyl group. As already emphasized, in ACE_C the lysine side chain of lisinopril forms a salt bridge with D377. Replacement of lisinopril's lysine by enalaprilat's alanine abolishes this salt bridge and results in reduced binding for the C domain, but increased binding for the N domain. The higher affinity of the enalaprilat for the C domain could be attributable to additional hydrophobic interactions of the alanyl group with the S1′ subsite of the C domain. As shown in Figure 4A and B), the alteration V380/T358 (ACE_C/ACE_N) results in a favorable hydrophobic interaction of the S1′ subsite (V380) with the P1′ group of the inhibitor in the C domain.

Keto-ACE: Keto-ACE (Scheme 1), is a ketomethylene derivative of the blocked tripeptide substrate Bz-Phe-Gly-Pro.[26] Recently, it has been reported that keto-ACE is a more potent inhibitor of the C domain in the hydrolysis of various substrates by somatic ACE.[7,27] The IC_{50N} for ACE_N was found to be 38 to 47 times higher than for ACE_C with AI and BK substrates. Docking calculations for keto-ACE in ACE_C and ACE_N produced the binding mode depicted in Figure 5. The estimated free energies of binding are consistent with the biologically determined affinities for the relevant domains ($E = -13.0$ and -12.5 kcal mol^{-1} for ACE_C and ACE_N, respectively). The pyrrolidine ring, the carboxyl and carbonyl groups of proline, and the phenyl ring are found to be in the same location as **I** in the crystal structure of the ACE–lisinopril complex and share common binding features for both domains (Table 1). The carbonyl oxygen of the benzamido group of keto-ACE forms a hydrogen bond with the backbone amide hydrogen of A356 in ACE_C and A334 in ACE_N and the benzamido amide proton is in close contact with the side chain of the zinc(II)-binding residues E411 in ACE_C and E389 in ACE_N. The key feature that provides a higher selectivity of keto-ACE for the C domain could be ascribed to the F391/Y369 alteration in the S2 subsite. As shown in Figure 5A, the benzyl ring is oriented for a stacking interaction with the aromatic side chain of F391, with the planes of the two rings nearly perpendicular. In the case of ACE_N, Y369 results in an unfavorable contact in the specific position of the S2 subsite (Figure 5B).

Ramiprilat: Ramiprilat (Scheme 1) closely resembles enalaprilat in its structure, though possessing an additional cyclopentane

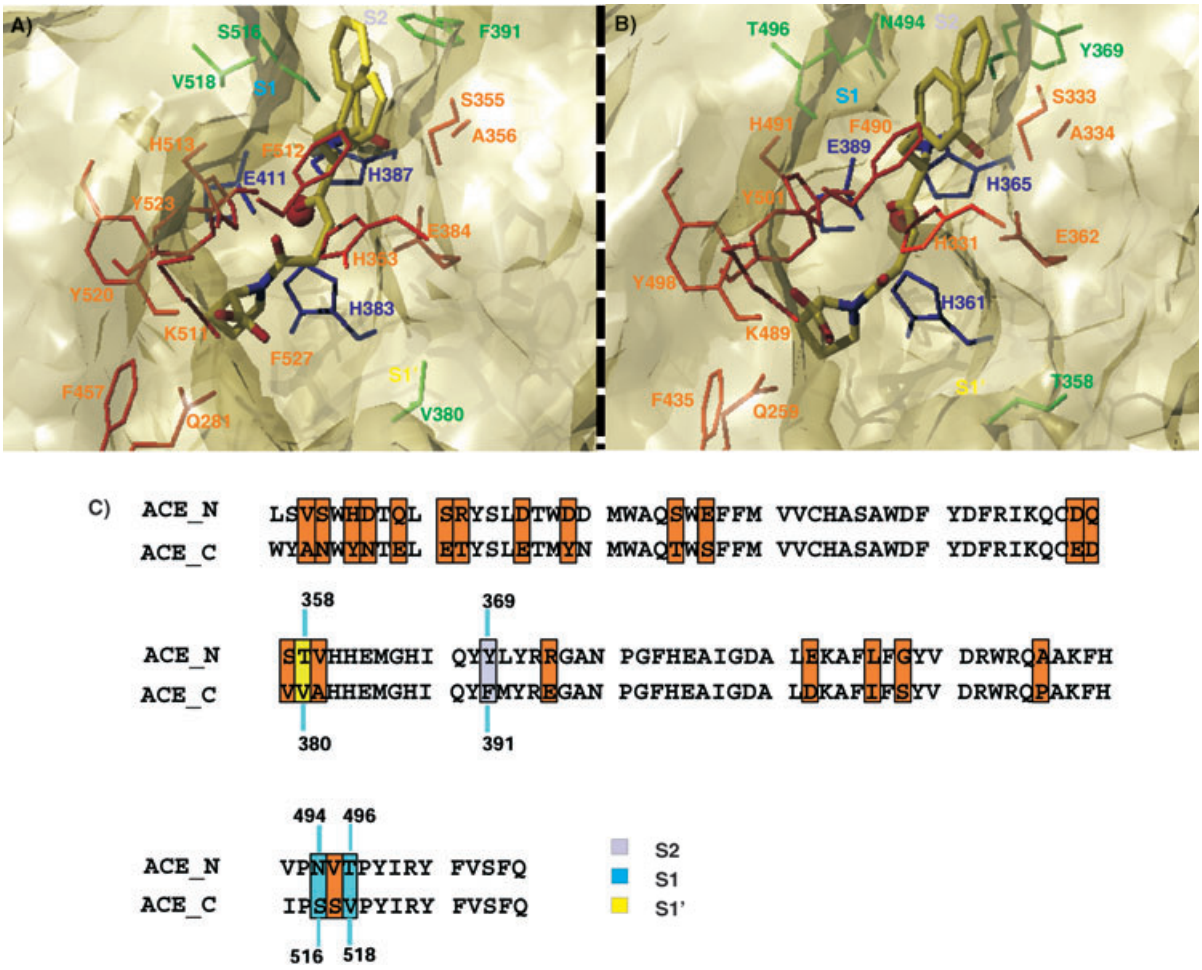

Figure 5. Binding of keto-ACE (**IV**) to A) the ACE_C and B) the ACE_N binding sites. C) Amino acid alignment of the residues of the two binding pockets of ACE_N and ACE_C for a cutoff of 10 Å radius around keto-ACE.

ring, which makes the molecule more lipophilic, whereas the shape of the molecule does not change apparently. Ramiprilat shares common binding features with enalaprilat (Figure 6), with a more favorable affinity for the C domain ($E = -14.8$ and -14.3 kcal mol^{-1} for ACE_C and ACE_N, respectively). This is attributed to additional hydrophobic interactions of the P1′ and P2′ groups of the inhibitor with V379 and V380 in the S1′ and S2′ subsites of ACE_C (altered to T358 and S357, respectively, in the ACE_N domain). Interestingly, the docking calculations revealed the presence of a hydrophobic patch provided by the aromatic rings of F457/F435, F527/F505, Y520/Y498, and Y523/Y501, interacting with the bicyclooctane ring system. This suggests a further explanation for the fact that sACE generally favors a bulky hydrophobic residue, such as isoleucine or phenylalanine, at the carboxy-terminal positions of substrate inhibitors.[3]

Perindoprilat: Perindoprilat closely resembles ramiprilat in structure (Scheme 1). It differs in its P1 group, having an alkyl chain, and also in P2′, having a hexahydroindoline (perhydroindole) group, similar to the bicyclooctane group of ramiprilat, that make the molecule more lipophilic. Docking calculations revealed a binding mode for **VI** (Figure 7) with similar affinities for both domains ($E = -15.2$ kcal mol^{-1} and -15.1 kcal mol^{-1} for the C- and the N domains, respectively). The alkyl group occupies the S1 enzyme subsite defined by the common residues S355/S333, F512/F490 (forming hydrophobic interactions), V518/T496, and S516/N494 in ACE_C/ACE_N. The V518/T496 alteration indicates a more favorable hydrophobic interaction with this specific subsite of the inhibitor in the C domain. In addition, the perhydroindole ring system interacts with the hydrophobic patch provided by the aromatic rings of F457/F435, F527/F505, and Y520/Y498 and Y523/Y501 (ACE_C/ACE_N). As in the case of ramiprilat, the V379/S357 alteration provides an additional hydrophobic interaction with the S2′ subsite in the C domain in relation to the relevant subsite in the N domain. These observations might explain the 40-fold increased C selectivity of perindoprilat.

ACE_C and ACE_N–quinaprilat complexes

Quinaprilat, closely resembling ramiprilat and enalaprilat in its structure, differs in the P2′ position due to the presence of a tetrahydroisoquinoline moiety (Scheme 1). The aromatic ring of this group, *as in ramiprilat and perindoprilat*, confers increased lipophilicity in the molecule. Docking calculations revealed a T-shaped hydrophobic interaction for this group with the F527/F505 side chain (Figure 8). The calculated free energies of binding for the complex of quinaprilat with the *s*ACE C and N domains were found to be -15.3 and -14.7 kcal mol^{-1}, respectively; this is in accordance with the biologically estimated inhibitor affinity, found to be 180 times more C-selective.[28] This result could be explained, as in the cases of ramiprilat and enalaprilat, in terms of additional hydrophobic interactions in the S1 and S2′ subsites of the C domain with the P1 and P2′

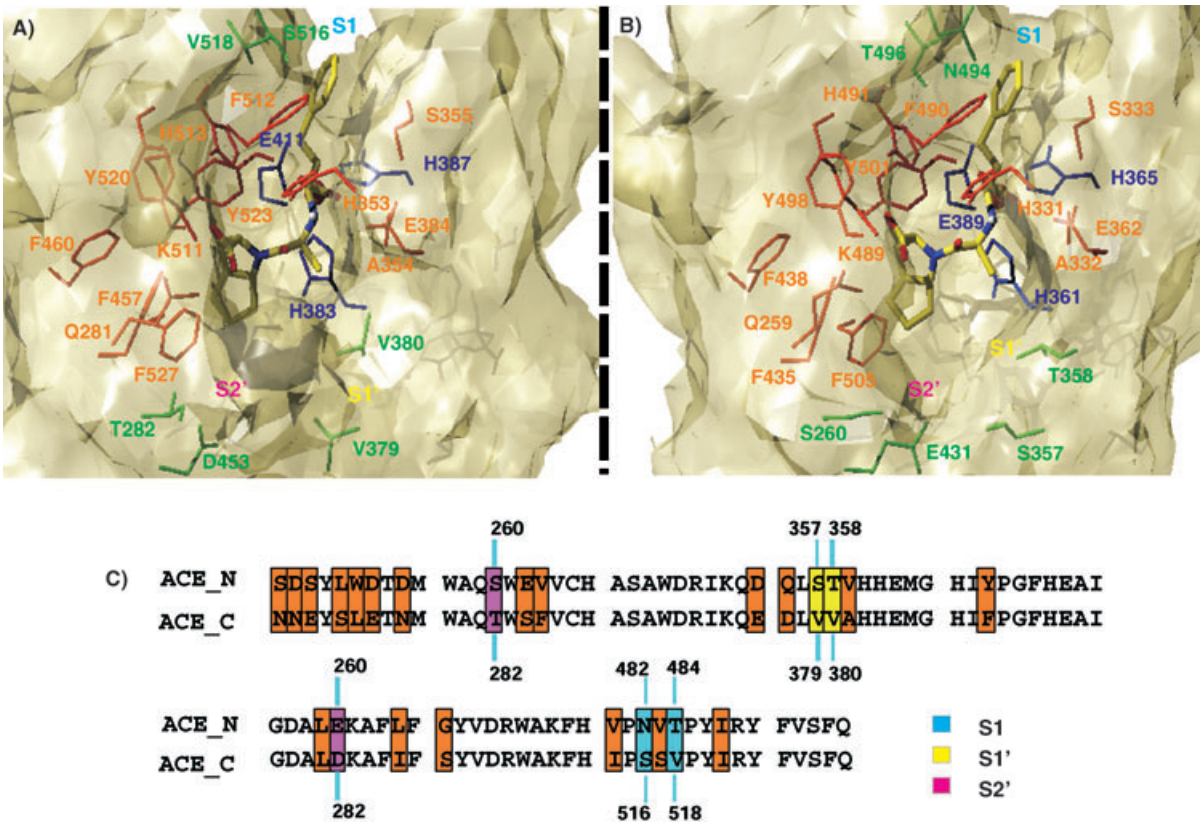

Figure 6. Binding of ramiprilat (**V**) to A) the ACE_C and B) the ACE_N binding sites. C) Amino acid alignment of the residues of the two binding pockets of ACE_N and ACE_C for a cutoff of 10 Å radius around ramiprilat.

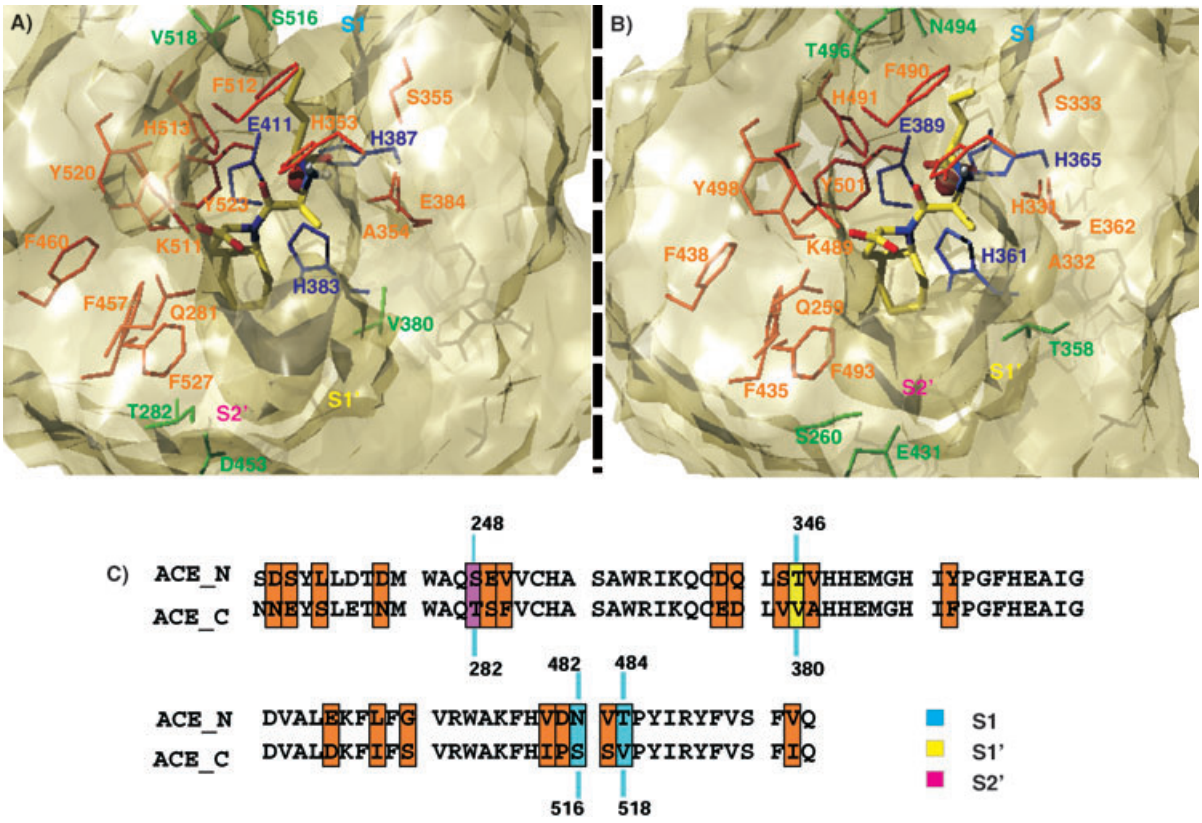

Figure 7. Binding of perindoprilat (**VI**) to A) the ACE_C and B) the ACE_N binding sites. C) Amino acid alignment of the residues of the two binding pockets of ACE_N and ACE_C for a cutoff of 10 Å radius around perindoprilat.

groups of the inhibitor, respectively. The weaker inhibitor activity for the N domain could be ascribed to the nonproductive accommodation of the P1 group in the S1 subsite. The amino acid residue N494, unique to the N domain and replaced by S516 (SSV) in the C domain, occurs in an *N*-glycosylation sequon (NVT); attachment of any glycan to this residue would therefore occlude this specific pocket.[29]

ACE_C– and ACE_N–phosphinic inhibitor complexes: the cases of fosinoprilat and RXP 407

The chemical structure of fosinoprilat is shown in Scheme 1 and, as would be expected, the phosphinyl group is the coordination site to the zinc(II) ion. The K_i values for inhibition of the hydrolysis of several substrates (e.g., Hip-His-Leu or Ang I), vary markedly according to the substrate used for the two domains;[6] fosinoprilat has K_i values of 0.02 and 0.07 nM for the inhibition of AcSDKP for the N- and the C domains, respectively, for example, whereas the same inhibitor displays K_i values of 2.78 and 0.48 nM with Hip-His-Leu as substrate for the two domains.

Fosinoprilat binds to the two domains with similar affinities ($E = -16.7$ and -16.5 kcal mol^{-1} for the C- and the N domains, respectively), it is located in the center of the typical binding pocket, and it shares common binding features (see Tables 1 and 2 and Figure 9). The benzyl ring in the phosphinyl terminal of the inhibitor is accommodated within the probable S1 subsite through aromatic stacking with F512/F490 (ACE_C numbering first) and hydrophobic interactions with V351/V329 and W357/W335, and is also in close contact with S355/S333 and K368/K346. In the same subsite of the enzyme the sequence alterations S516/N494 and V518/T496 can be observed. As shown in Figure 9, the optimum accommodation of the benzyl group is adopted in the ACE_N S1 subsite, as the S516/N494 alteration could result in a favorable cation–π interaction between the benzyl ring of the ligand and the asparagine group of the enzyme.

A major difference observed for the binding modes of the inhibitor in the two domains is the orientation of the cyclohexane group; in the N domain it is perpendicular to the pyrrolidine ring of proline ($\approx 90°$) and in the C domain it is parallel. This fact could be explained by the D453/E431 and T282/S260 alterations (ACE_C/ACE_N) observed in the S2′ subsite. In ACE_N these alterations result in increases in the sizes of the specific side chains, and lead to a reduction of the available space in the S2′ subsite. Furthermore, the V379/S357 and V380/T358 alterations in the same subsite (Figure 9) result in the development of favorable hydrophobic interactions between the cyclohexane group and V379 and V380 in the ACE_C domain. These observations suggest that a bulky P2′ group confers C selectivity.

RXP 407: RXP 407, or Ac-Asp-Phe-ψ(PO_2-CH_2)Ala-Ala-NH_2 (Scheme 1), is the most important ACE_N-selective inhibitor, pioneered by Corvol and collaborators.[9] The X-ray structure of

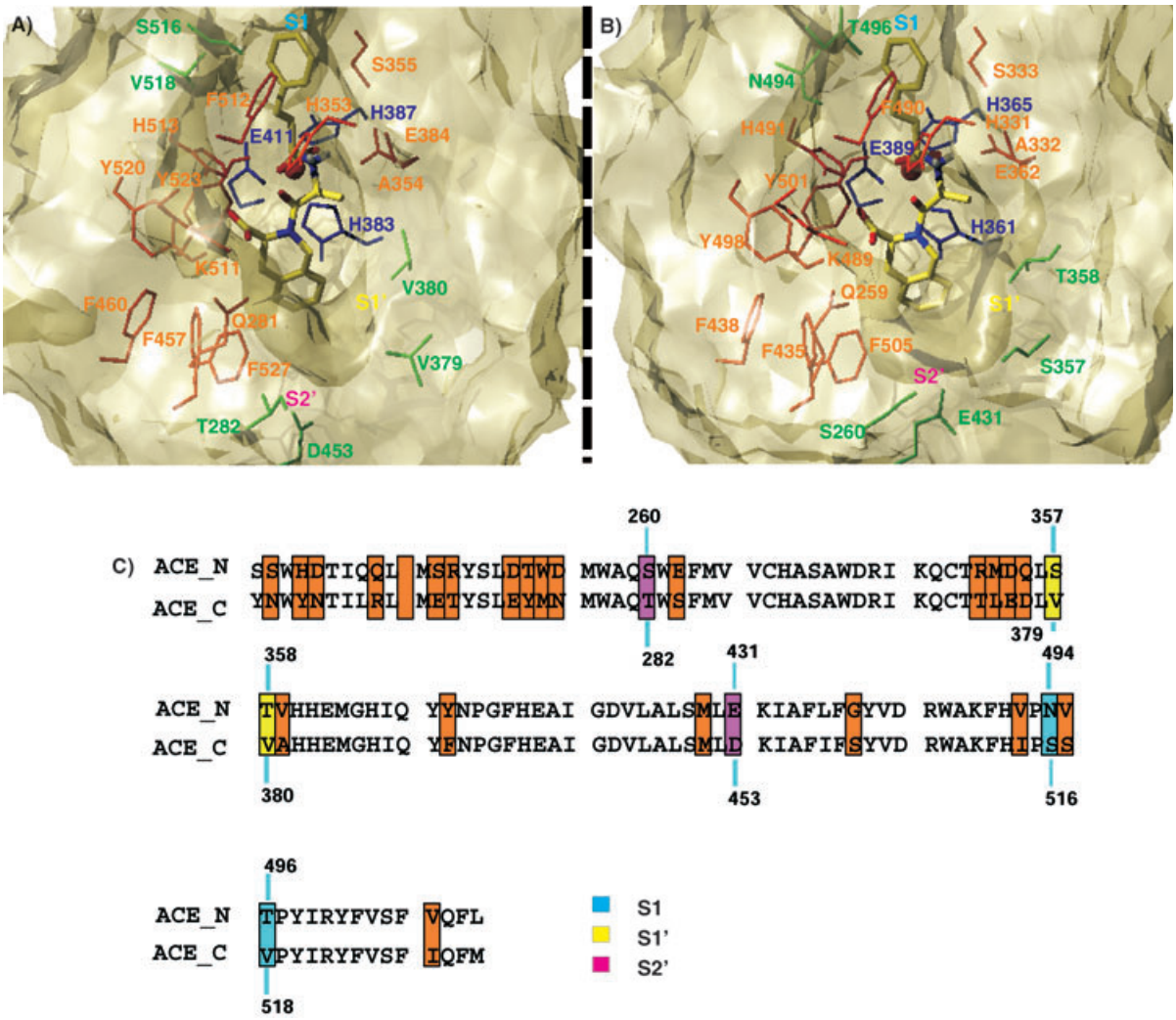

Figure 8. Binding of quinaprilat (**VII**) to A) the ACE_C and B) the ACE_N binding sites. C) Amino acid alignment of the residues of the two binding pockets of ACE_N and ACE_C for a cutoff of 10 Å radius around quinaprilat.

the close analogue PKF, a phosphinic pseudopeptide analogue (carbobenzoxy-Pro-Lys-Phe-$\psi(PO_2\text{-}CH_2)$-Ala-Pro-OMe), has been resolved at 2.14 Å as a complex with astacin (Figure S6).[30] Figure 10 depicts an overlay of lisinopril (in the *t*ACE–lisinopril complex, colored in red and cyan, respectively) with PKF (in the astacin–PKF complex, colored in green and pale green, respectively) and catalytic residues from both proteins. The alignment was performed on the HEXXH motif of the two proteins and reveals a close homology of the binding grooves. The superposition reveals a common space rearrangement of specific pharmacophore groups (depicted in orange dotted circles) for lisinopril and the PKF inhibitors of *t*ACE and astacin, respectively. A model of RXP 407 based on these observations has been constructed and the common chemical groups of the two structures were further refined.

Docking calculations for RXP 407 in the ACE_C and ACE_N domains resulted in the binding mode depicted in Figure 11. The estimated free energies of binding ($E = -14$ and -17 kcal mol^{-1} for ACE_C and ACE_N, respectively) are consistent with the biologically estimated affinities for the relevant domains (with K_i values of 75 000 nM for the C domain and 7 nM for the N domain; Tables 1 and 2). The carbonyl oxygen of the aspartate group of RXP 407 forms hydrogen bonds with the backbone amide hydrogens of A356 in ACE_C and A334 in ACE_N. The carboxyl group of the side chain of aspartate in the inhibitor is hydrogen-bonded with the side chain of R500/R522 (ACE_N/ACE_C) in the S2 subsite (R522 is important for the C domain, since it is the chloride-binding residue and the direct distortion of this interaction could have an effect in the reduction of the inhibitor binding[21]). Docking calculations also favored a second cluster of the complex with the side chain of the aspartyl group to form van der Waals interactions with H410 and H388 in ACE_C and ACE_N (data not shown). The phenyl group in the P1 position enters into the same interactions with the S1 subsites of ACE_C and ACE_N as in the cases of lisinopril, ramiprilat, quinaprilat, and enalaprilat. The amide proton of the phenylalanine group is in close contact with the side chains of the zinc(II)-binding residues E411 in ACE_C and E389 in ACE_N (as in the case of keto-ACE). The alanyl group of the P1′ subsite engages in the same interactions as devel-

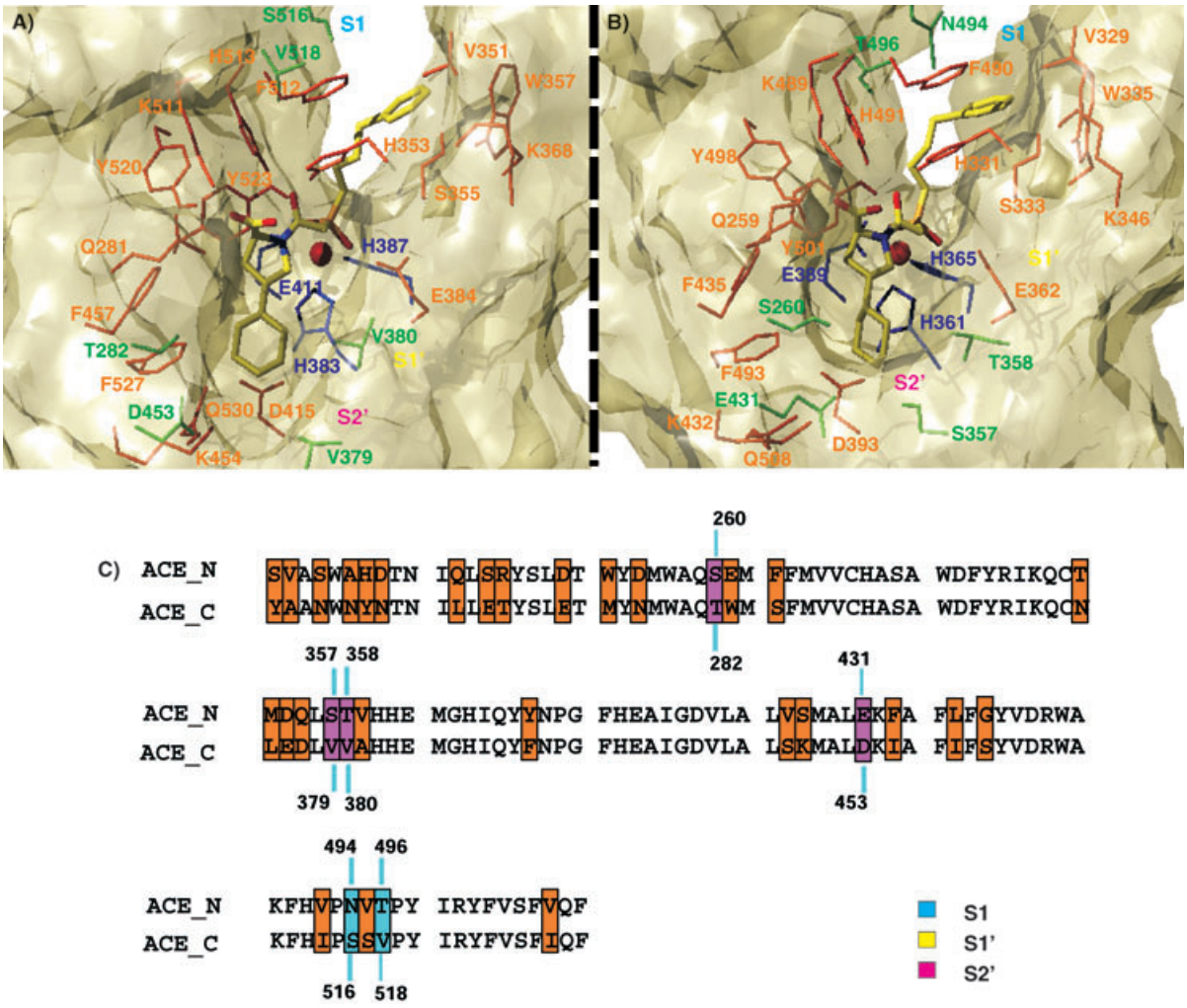

Figure 9. Binding of fosinoprilat (**VIII**) to A) the ACE_C and B) the ACE_N binding sites. C) Amino acid alignment of the residues of the two binding pockets of ACE_N and ACE_C for a cutoff of 10 Å radius around fosinoprilat.

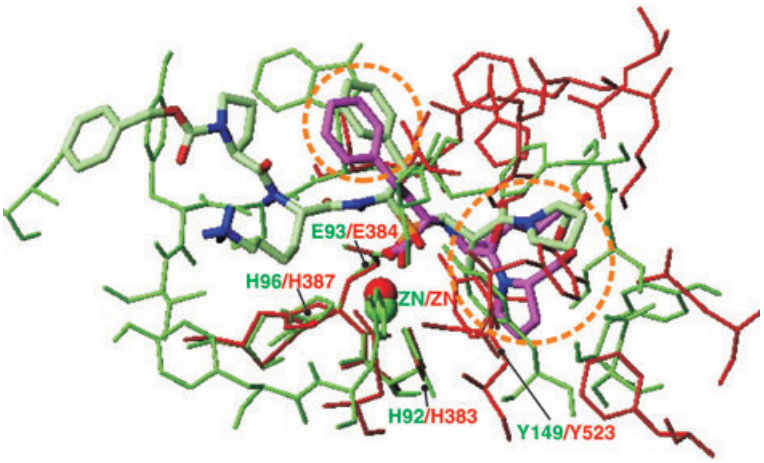

Figure 10. Superposition of PKF (green, bold line) in the binding site of astacin (green) with lisinopril (magenta, bold line) in the binding site of tACE (red). A cutoff of 4 Å radius has been used for the enzyme residues around the inhibitor molecules.

oped with enalaprilat, perindoprilat, quinaprilat, and ramiprilat, and the same applies for the corresponding carbonyl group. An interesting feature is the positioning of the alanyl group of the P2′ subsite, located in the hydrophobic patch provided by the aromatic rings of F457/F435, F527/F505, and Y520/Y498 and Y523/Y501 (ACE_C/ACE_N), closely resembling the positioning of the C-terminal leucine group of AI. The C-terminal carboxyamide group, both in ACE_C and ACE_N, makes favorable interactions with K511/K489 and Y520/Y498 (ACE_N/ACE_C).

The higher selectivity for RXP 407 for the N domain could be attributable, firstly, to the F391/Y369 alteration in the S2 subsite. As shown in Figure 11 A, the amide proton of the aspartate moiety in ACE_N appears to form a hydrogen bond with the side chain of Y369, in contrast to the case in ACE_C, where a phenylalanine group is substituted (F391). Secondly, the *N*-acetyl carbonyl group favors hydrogen bond interactions with R381, in contrast with the repulsive forces developed in the case of ACE_C due

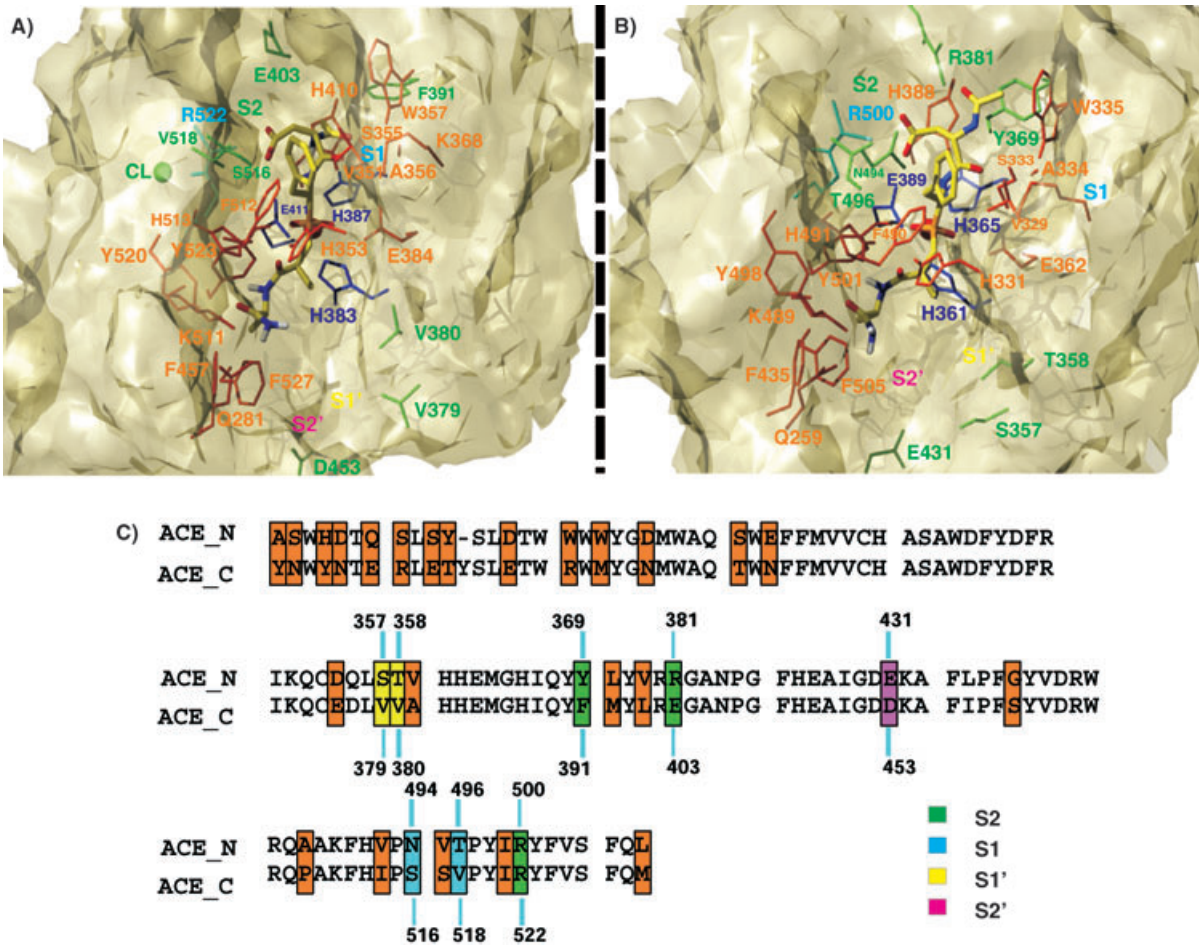

Figure 11. Binding of RXP 407 (**IX**) to A) the ACE_C and B) the ACE_N binding sites. C) Amino acid alignment of the residues of the two binding pockets of ACE_N and ACE_C for a cutoff of 10 Å radius around RXP 407.

to the E403 alteration. Thirdly, the amine group of the C-terminal carboxyamide moiety interacts with the side chain of E431 in ACE_N. The alteration to D453 in ACE_C would result in an increase in the distance from the side chain of D453 to the amine group of RXP 407. The ACE_N selectivity of RXP 407 is therefore based on the presence of a C-terminal carboxyamide group, an aspartic side chain in the P2 position of the inhibitor, and an N-acetyl group. These structural features are well tolerated by the N-terminal active site, but act repulsively in the binding of the inhibitor to the C-terminal active site of ACE. Structure–activity relationships have long suggested that a free C-terminal carboxylate group in the P2′ position of the inhibitor is an absolute requisite for the preparation of potent inhibitors of ACE,[31] which explains why free carboxylate groups in the P2′ position have routinely been incorporated in ACE inhibitor structures over the last two decades. This has probably impeded the discovery of selective inhibitors of the N-terminal active site of ACE.

Our docking calculations were also able to provide an explanation of structure–activity studies of phosphinic tetrapeptides indicating that an aspartic side chain and an N-acetyl group, located in the P2 position, together with a C-terminal carboxyamide group, contribute to selectivity for the N domain.[9] Thus, H_2N-Asp-Phe-ψ(PO_2-CH_2)-Ala-Ala-NH_2 is more selective for the N domain (K_i for ACE_N = 5 nM, K_i for ACE_C = 800 nM) due to interactions of the N-terminal amino group with Y369 and of the C-terminal amino group with E431, which are absent in the C domain. The N selectivity of Ac-Asp-Phe-ψ(PO_2-CH_2)-Ala-Ala-NH_2 (K_i for ACE_N = 15 nM, K_i for ACE_C = 200 nM) could also be interpreted by hydrogen bonding of the amide proton of the P2 group (aspartate) with Y369 and of the carbonyl group of the N-acetyl group with R381, unique to the N domain. However, Ac-Asp-Phe-ψ(PO_2-CH_2)-Ala-Ala-OH displays similar inhibitory potencies for the two domains (K_i for ACE_N = 2 nM, K_i for ACE_C = 7 nM),[10] due to the absence of the carboxamido group and thus the interaction with the E431 group of ACE_N.

Pharmacophore refinement and guidelines for structure-based ligand design

The free energies of binding (E) for the relevant inhibitors of the two ACE domains, as estimated by use of the AutoDock program, are consistent with the experimentally determined literature inhibition data (Tables 1 and 2). In the ACE_C domain, lisinopril was found to have a lower estimated K_i than

enalaprilat, which in turn has a lower K_i value than captopril. This follows the observed inhibitory potencies given in the literature (for lisinopril, enalaprilat, and captopril, $K_i = 0.24$, 0.63, and 1.40 nM, respectively[3]). Of these inhibitors, lisinopril, enalaprilat, and keto-ACE were calculated to have lower inhibitor potencies for the ACE_N domain whereas the reverse was observed for RXP 407. This is in accordance with the literature data (Tables 1 and 2). In addition, the docking calculations suggested that perindoprilat and quinaprilat should be more C-selective; this is confirmed by results from radioligand-binding studies, which indicated that both perindoprilat and quinaprilat are 45–180 times more C-selective.[28] However, comparison beyond these general considerations is not feasible, as it has been reported that the active sites of the enzyme may interact with each other,[32] which implies spatial proximity and contacts between the two domains. Nevertheless, this is a good performance for an empirical free energy function, as it allows a reasonably accurate estimation of the affinity range as reported in the literature.[33]

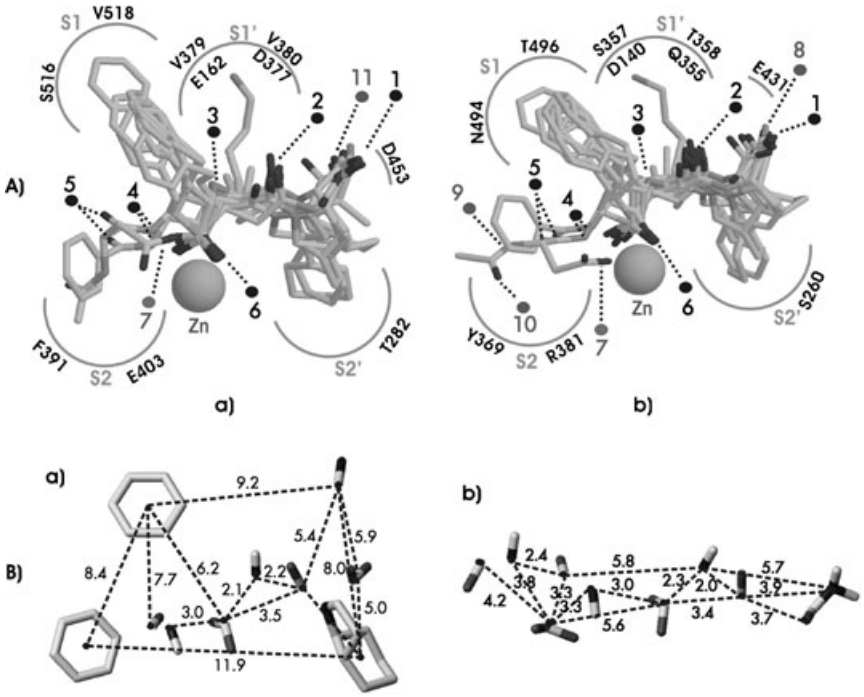

Figure 12. A) Overlay of putative bioactive conformations of compounds **I**–**IX** bound to a) ACE_C and b) ACE_N. Superposition was performed by aligning the ACE_C and ACE_N domains. The numbering 1–5 denotes the ACE_C/ACE_N residues involved in hydrogen bonds to the highlighted portion of the inhibitor, 6 denotes the interaction point with the chloride-binding arginine, and 7–9 are hydrogen bonding contacts appearing only in the case of the N domain (**1**: Q281/Q259, K511/K489, Y520/Y498, **2**: H353/H331, H513/H491, **3**: A354/A332, **4**: E411/E389, **5**: A356/334, **6**: Y523/Y501, **7**: R522/R500, **8**: E431, Q281/Q259 **9**: Y369, **10**: R381, **11**: Q281/Q259). Alterations observed in the four subsites of the ACE_C/ACE_N are: S1: V516/N494, V518/T496, S2: F391/Y369, E403/R381, S1′: V379/S357, V380/T358, E162/D140, D377/Q355, S2′: D453/E431, T282/S260. B) Distances between the pharmacophoric points calculated as averages over the ACE_C- and ACE_N-bound conformations of compounds **I**–**IX**, describing the spatial arrangements of functional groups necessary for binding.

Comparison of the inhibitor structures in their unbound and bound states to the ACE_C and ACE_N domains reveals common structural features for their backbones and zinc(II)-binding sites and some differences in the orientations of the side chains of the P2′, P1, and P2 subsites (Figure S2 in the Supporting Information).

Figure 12A shows an overlay of the inhibitors **I**–**IX** bound i) to ACE_C, and ii) to ACE_N domains. Alterations observed in the four subsites of the ACE_C/ACE_N are: S1: V516/N494, V518/T496, S2: F391/Y369, E403/R381, S1′: D377/Q355, E162/D140, V379/S357, V380/T358, and S2′: D463/E431, T282/S260. The main interaction sites observed for the C domain (Figure 12A) consist of a bulky hydrophobic group in P2′, a carboxyl group in the C terminus, a basic group in P1′, and the benzyl groups in the P1 and P2 positions. In the N domain, the main interaction points consist of a hydrophobic residue in P2′, a carboxamido group in the C-terminus, an aspartic in P2, and a carbonyl group in the N terminus (Figure 12Ab). The molecular alignment illustrated in Figure 12A and based on the selective C-domain inhibitor keto-ACE and the selective N-domain inhibitor RXP 407 suggest the existence of five hydrogen bond acceptor sites (1, 2, 4, 5, and 10) and one hydrogen bond donor site (3) necessary for tight binding of the inhibitor in the C domain. In the N domain, the additional hydrogen bond acceptor site (9) and two hydrogen bond donor sites (7, 8) further refine the ligand selectivity pharmacophore model. In addition to these sites, the interaction of the aspartyl side chain (6) of the inhibitor with an arginine confers N selectivity (in the case of the C domain this arginine is a necessary chloride-binding residue).

Careful examination of the free energies of binding for ramiprilat, quinaprilat, fosinoprilat, and perindoprilat (Tables 1 and 2) and the molecular alignment of Figure 12A reveal that in the S2′ subsite, consisting of a hydrophobic patch, a bulky P2′ group confers C selectivity, further refining the pharmacophore model for a C-selective inhibitor.

Previous investigation of the substrate specificity requirements for ACE_C and ACE_N domains by use of quenched fluorescence peptides suggested the importance of hydroxy-containing amino acids at the P2 position for N domain specificity; Ser and Asp at P2 and P1, respectively, thus have synergic effects in determining the differential specificity for the N domain in relation to the C domain.[34] This fact could be interpreted through the current detailed differential mapping of the two enzyme domains, in terms of favorable interactions of Ser (P2) with the Y369 of the S2 subsite of ACE_N (F391 in

ACE_C) and Asp (P1) with R500 of the S1 subsite in ACE_N (R522 in ACE_C is a chloride-binding residue). In addition, it has also been reported that Abz-GFSPFFQ-EDDnp (F in the P1 subsite) is preferentially hydrolyzed by the C domain, while Abz-GFSPFQQ-EDDnp (Q in the P1 subsite) exhibits a higher N domain specificity. This higher specificity of the C domain for F in P1 could be explained, as the S1 subsite in ACE_N is a potent glycosylation site, resulting in occlusion of the site, and by the favorable interaction with V518 (T496 in ACE_N). The higher specificity of the N domain for Q in P1 could be explained in terms of the development of potent electrostatic interactions with N494, altered to S516 in the C domain.

The distances between the pharmacophoric points calculated as averages over the bound conformations of compounds **I**–**IX** for ACE_C and ACE_N are shown in Figure 12B. If these docking results are taken together, a potent selective pharmacophore model for ACE_C and ACE_N could be proposed (Figure 12B).

Conclusion

The recent publication of the X-ray structures of *t*ACE and drosophila AnCE in complexes with potent ligands has allowed us to determine the receptor-bound conformations and the mutual alignments of several representative ACE inhibitors. All compounds exhibit similar binding modes and therefore make up an ideal target for systematic variation of a substituent.

In ACE_C and ACE_N, the common interactions responsible for tight binding of the inhibitors are: i) coordination of Zn^{II} with the carboxylate, phosphinic, or thiol oxygen(s)/sulfur of the substrate and hydrogen bonding of (6) to Y523/Y501, ii) a hydrogen bond of (1) in the inhibitor with Y520/Y498 and electrostatic interaction with K511/K489, iii) hydrogen bonding of (2) with H513/H491 and H353/H331, iv) hydrogen bonding of (3) with the carbonyl group of A354/A332, and v) hydrogen bonding of (5) with the amide proton of A356/A334.

The interactions governing the ligand–receptor recognition process in the ACE_C domain are: i) a salt bridge between D377, E162, and the NH_2 group of the side chain of the ligand in the P1′ position, ii) a hydrogen bond of the carboxyl oxygen of (1) with Q281, iii) the presence of bulky hydrophobic groups in the P1 and P2′ sites, and iv) a stacking interaction of the aromatic side chain of F391 with a benzyl group in the P2 position.

In ACE_N the interactions suggesting selectivity for the recognition process are: i) a hydrogen bond of the amido group (8) with E431, ii) a salt bridge of the carboxyl group of P2(7) with R500, iii) a hydrogen bond of (9) with Y369, and iv) a hydrogen bond of (10) with R381.

The knowledge reported here might therefore form a starting point for the rational design of novel, potent domain-specific inhibitors, improving on the current class of ACE inhibitors, which already find widespread application in the treatment of cardiovascular and renal diseases. The next step in this line of research will be the design of lead compounds based on our refined pharmacophore model and on the active site topology.

Computational Methods

The model of the N-catalytic domain of *s*ACE (ACE_N), based on the crystal structure of the testis isoform of ACE (pdbid 1O8A), is described elsewhere.[21] In this study, the inhibitor-bound structure of ACE_N (30 models) was constructed through comparative modeling by use of MODELER 6.2v[35] based on the recently solved crystal structure of the *t*ACE–lisinopril complex (pdbid: 1O86[19]). Of the 30 models, the one with the lowest energy[36] and best stereochemistry was selected.[37] The root-mean-square deviation of all backbone atoms was found to be 0.19 Å for the ACE_C–lisinopril complex, with no changes in secondary assignments. We then used two protein structure verification methods that characterize the environments of residues to assess the ACE_N model relative to the X-ray ACE_C structure. Both the PROFILER3D[38] and ERRAT[39] programs gave comparable scores for ACE_N and ACE_C. Structure superposition of *t*ACE in complexation with lisinopril (pdbid: 1O86),[19] with AnCE in complex with lisinopril (pdbid: 1 J36)[22] and with ACE2 in complex with the MLN-4760 inhibitor (pdbid: 1R4L)[40] gave rmsds of 1.03 Å and 1.22 Å, respectively (Figure S4 in the Supporting Information). Interestingly, structure alignment of the active sites of the discussed inhibitor-bound forms of the enzymes *t*ACE(ACE_C) with AnCE and ACE2 gave rmsds of 0.43 Å and 0.69 Å respectively, with the three inhibitors fully superimposed (Figure S5 in the Supporting Information). Therefore, despite a profound conformational change in the unbound and inhibitor-bound forms of ACE2,[40] it can be concluded that angiotensin converting enzyme retains very similar overall structural features of the inhibitor-bound form even in different isoforms where sequence diversity is high. Thus, since the sequence homology between ACE_N and ACE_C is $\approx$55%, high accuracy could be expected for the constructed model of the inhibitor-bound form of the ACE_N domain based on the crystal structure of the *t*ACE–lisinopril complex.[19]

Docking calculations of ligands **I**–**IX** (Scheme 1) to ACE_N and ACE_C were carried out by use of the provided empirical free energy function and the Lamarckian Genetic Algorithm (LGA) method[41] as implemented in the AutoDock program, by application of a protocol with an initial population of 50 randomly placed individuals, a maximum number of 1.5×10^6 energy evaluations, a mutation rate of 0.01, a crossover rate of 0.80, and an elitism value of 1. For the local search, the Solis and Wets algorithm was applied with the use of a maximum of 300 interactions per local search. Fifty independent docking runs were carried out for each ligand. Results differing by less than 1 Å in positional root-mean-square deviation (rmsd) were clustered together and represented by the most favorable free energy of binding. For the protein setup, Kollman united atom partial charges were assigned, and all waters were removed. Solvation parameters were added to the final protein file with the aid of the ADDSOL utility in the AutoDock program. The grid maps, representing the protein in the docking process, were calculated with AutoGrid. The grids were chosen to be large enough to include a significant part of the protein around the binding site. In all cases we used grid maps with $61\times61\times61$ points with a grid point spacing of 0.375 Å. The center of the grid was set to be coincident with the mass center of the ligand in the crystal complex. As has been mentioned, comparisons of the structures of the complex and the free enzyme of *t*ACE and drosophila AnCE[22] show that the inhibitor binding does not induce a significant rearrangement of the active site residues, so the system was not further energy minimized.

The atomic coordinates of lisinopril and captopril and enalaprilat were taken from their complexes with *t*ACE.[19,20] The structures of fosinoprilat, quinaprilat, ramiprilat, enalaprilat, peridoprilat, and

keto-ACE were retrieved from the Cambridge Crystallographic Database (CCD). The phosphinic ligand RXP 407 was constructed with use of the PRODRG server,[42] whereas the torsion angles were further refined manually, on the basis of the common molecular parts of the relevant phosphinic peptide PKF bound to astacin (pdbid: 1QIJ[30]). All the relevant torsion angles were regarded as flexible during the docking process, thus allowing a search of the conformational space.

Acknowledgements

Dr. Peggy Graber (The Scripps Research Institute, Molecular Graphics Laboratory, Department of Molecular Biology) is gratefully acknowledged for assistance with the Autodock 3.0.5 software. A.G.T. acknowledges an award from the "Leonidas Zerbas" Foundation. This research was funded by the "Heraklitos" program of the Operational Program for Education and Initial Vocational Training of the Hellenic Ministry of Education under the 3rd Community Support Framework and the European Social Fund.

Keywords: angiotensin I converting enzyme · drug design · inhibitors · metalloproteins · molecular modeling · molecular recognition

[1] F. Soubrier, F. Alhenc-Gelas, C. Hubert, J. Allegrini, M. John, G. Tregear, P. Corvol, *Proc. Natl. Acad. Sci. USA* **1988**, *85*, 9386 – 9390.
[2] L. Wei, F. Alhenc-Gelas, P. Corvol, E. Clauser, *J. Biol. Chem.* **1991**, *266*, 9002 – 9008.
[3] L. Wei, E. Clauser, F. Alhenc-Gelas, P. Corvol, *J. Biol. Chem.* **1992**, *267*, 13398 – 13405.
[4] E. Jaspard, L. Wei, F. Alhenc-Gelas, *J. Biol. Chem.* **1993**, *268*, 9496 – 9503.
[5] P. A. Deddish, L. X. Wang, H. L. Jackman, B. Michel, J. Wang, R. A. Skidgel, E. G. Erdos, *J. Pharmacol. Exp. Ther.* **1996**, 279, 1582 – 1589.
[6] A. Michaud, T. A. Williams, M. T. Chauvet, P. Corvol, *Mol. Pharmacol.* **1997**, 51, 1070 – 1076.
[7] P. A. Deddish, B. Marcic, H. L. Jackman, H. Z. Wang, R. A. Skidgel, E. G. Erdos, *Hypertension* **1998**, 31, 912 – 917.
[8] A. Rousseau, A. Michaud, M. T. Chauvet, M. Lenfant, P. Corvol, *J. Biol. Chem.* **1995**, *270*, 3656 – 3661.
[9] V. Dive, J. Cotton, A. Yiotakis, A. Michaud, S. Vassiliou, J. Jiracek, G. Vazeux, M. T. Chauvet, P. Cuniasse, P. Corvol, *Proc. Natl. Acad. Sci. USA* **1999**, *96*, 4330 – 4335.
[10] M. R. Ehlers, J. F. Riordan, *Biochemistry* **1991**, *30*, 7118 – 7126.
[11] M. Azizi, A. Rousseau, E. Ezan, T. T. Guyene, S. Michelet, J. M. Grognet, M. Lenfant, P. Corvol, J. Menard, *J. Clin. Invest.* **1996**, 97, 839 – 844.
[12] F. Soubrier, L. Wei, C. Hubert, E. Clauser, F. Alhenc-Gelas, P. Corvol, *J. Hypertens.* **1993**, *11*, 599 – 604.
[13] K. J. Rieger, N. Saez-Servent, M. P. Papet, J. Wdzieczak-Bakala, J. L. Morgat, J. Thierry, W. Voelter, M. Lenfant, *Biochem. J.* **1993**, *296*(2), 373 – 378.
[14] J. Menard, A. A. Patchett, *Adv. Protein Chem.* **2001**, *56*, 13 – 75.
[15] R. Candido, K. A. Jandeleit-Dahm, Z. Cao, S. P. Nesteroff, W. C. Burns, S. M. Twigg, R. J. Dilley, M. E. Cooper, T. J. Allen, *Circulation* **2002**, 106, 246 – 253.
[16] M. A. Zaman, S. Oparil, D. A. Calhoun, *Nat. Rev. Drug Discovery* **2002**, *1*, 621 – 636.
[17] D. Mayer, C. B. Naylor, I. Motoc, G. R. Marshall, *J. Comput.-Aided Mol. Des.* **1987**, *1*, 3 – 16.
[18] C. L. Waller, G. R. Marshall, *J. Med. Chem.* **1993**, *36*, 2390 – 2403.
[19] R. Natesh, S. L. Schwager, E. D. Sturrock, K. R. Acharya, *Nature* **2003**, *421*, 551 – 554.
[20] R. Natesh, S. L. Schwager, H. R. Evans, E. D. Sturrock, K. R. Acharya, *Biochemistry* **2004**, *43*, 8718 – 8724.
[21] A. G. Tzakos, A. S. Galanis, G. A. Spyroulias, P. Cordopatis, E. Manessi-Zoupa, I. P. Gerothanassis, *Protein Eng.* **2003**, 16, 993 – 1003.
[22] H. M. Kim, D. R. Shin, O. J. Yoo, H. Lee, J. O. Lee, *FEBS Lett.* **2003**, *538*, 65 – 70.
[23] M. Fernandez, X. Liu, M. A. Wouters, S. Heyberger, A. Husain, *J. Biol. Chem.* **2001**, *276*, 4998 – 5004.
[24] T. A. Williams, A. Michaud, X. Houard, M. T. Chauvet, F. Soubrier, P. Corvol, *Biochem. J.* **1996**, *318*, 125 – 131.
[25] S. H. Ferreira, L. H. Greene, V. A. Alabaster, Y. S. Bakhle, J. R. Vane, *Nature* **1970**, *225*, 379 – 380.
[26] R. G. Almquist, W. R. Chao, M. E. Ellis, H. L. Johnson, *J. Med. Chem.* **1980**, *23*, 1392 – 1398.
[27] J. A. Weare, T. A. Stewart, J. T. Gafford, E. G. Erdos, *Hypertension* **1981**, 3, I50 – 53.
[28] R. B. Perich, B. Jackson, C. I. Johnston, *Eur. J. Pharmacol.* **1994**, 266, 201 – 211.
[29] K. R. Acharya, E. D. Sturrock, J. F. Riordan, M. R. Ehlers, *Nat. Rev. Drug Discovery* **2003**, *2*, 891 – 902.
[30] F. Grams, V. Dive, A. Yiotakis, I. Yiallouros, S. Vassiliou, R. Zwilling, W. Bode, W. Stocker, *Nat. Struct. Biol.* **1996**, *3*, 671 – 675.
[31] M. A. Ondetti, B. Rubin, D. W. Cushman, *Science* **1977**, *196*, 441 – 444.
[32] P. V. Binevski, E. A. Sizova, V. F. Pozdnev, O. A. Kost, *FEBS Lett.* **2003**, *550*, 84 – 88.
[33] L. Marinelli, A. Lavecchia, K. E. Gottschalk, E. Novellino, H. Kessler, *J. Med. Chem.* **2003**, *46*, 4393 – 4404.
[34] M. C. Araujo, R. L. Melo, M. H. Cesari, M. A. Juliano, L. Juliano, A. K. Carmona, *Biochemistry* **2000**, *39*, 8519 – 8525.
[35] A. Sali, L. Potterton, F. Yuan, H. van Vlijmen, M. Karplus, *Proteins* **1995**, 23, 318 – 326.
[36] M. J. Sippl, *Proteins* **1993**, *17*, 355 – 362.
[37] R. A. Laskowski, M. W. MacArthur, J. M. Thornton, *Curr. Opin. Struct. Biol.* **1998**, *8*, 631 – 639.
[38] R. Luthy, J. U. Bowie, D. Eisenberg, *Nature* **1992**, *356*, 83 – 85.
[39] C. Colovos, T. O. Yeates, *Protein Sci.* **1993**, *2*, 1511 – 1519.
[40] P. Towler, B. Staker, S. G. Prasad, S. Menon, J. Tang, T. Parsons, D. Ryan, M. Fisher, D. Williams, N. A. Dales, M. A. Patane, M. W. Pantoliano, *J. Biol. Chem.* **2004**, *279*, 17996 – 18007.
[41] D. S. Goodsell, G. M. Morris, A. J. Olson, *J. Mol. Recognit.* **1996**, *9*, 1 – 5.
[42] D. M. van Aalten, R. Bywater, J. B. Findlay, M. Hendlich, R. W. Hooft, G. Vriend, *J. Comput.-Aided Mol. Des.* **1996**, *10*, 255 – 262.

Received: October 28, 2004

